$$I_3 = [\{M_\infty z^{1/2}/(2\lambda\cos\theta)\}\{-H\sin\theta\cos\theta$$
$$+(z-3a)(\sin\theta\cos\theta-\lambda H(\cos^2\theta+\cos 2\theta))/(3b)$$
$$+(3z^2-10az+15a^2)(\cos^2\theta+\cos 2\theta)\cdot\lambda/(15b^2)\}]_{z=a+b}^{z=a-b}$$
$$J_1 = M_\infty \sin\theta\cdot H^2 + M_\infty(\sin\theta-2\lambda H\cos\theta)/3.0$$
$$J_2 = [\{-2z^{3/2}/(3b)\}\{H^2/4.0+H(5a-3z)/(10b)$$
$$+(15z^2-42az+35a^2)/(140b^2)\}]_{z=a+b}^{z=a-b}$$
$$J_3 = [\{-z^{1/2}/(\lambda\cos\theta)\}\{(H^2\sin\theta)/4.0$$
$$-H(\sin\theta-\lambda H\cos\theta)(z-3a)/(6b)$$
$$+(\sin\theta-4\lambda H\cos\theta)(3z^2-10az+15a^2)/(60b^2)$$
$$+\lambda(5z^3-21z^2a+35za^2-35a^3)\cos\theta/(70b^3)\}]_{z=a+b}^{z=a-b}$$

In the preceding equations,

$H = 1-2h\cos^2\theta$, $a = [4/(r+1)]^2 + M_\infty^2\sin^2\theta$, and $b = \lambda M_\infty^2 \sin 2\theta$. Figure 3 compares results for plane wedge with Hui's theory and also with convex (λ positive) and concave (λ negative) nonplanar wedges.

Conclusion

Figure 2 demonstrates the theory's wide application range, in incidence and Mach number, for planar and nonplanar surfaces. It is free from the restrictions of Lighthill's[2] theory ($\alpha \ll 1$, $M_\infty \alpha \leq 1$) and Miles'[11] theory ($\alpha \ll 1$, $M_\infty \alpha \gg 1$). Figure 3 shows that the effect of convexity in nonplanar wedges is to decrease stiffness and shift damping minima towards the leading edge. Differences with Hui's theory for the plane wedge are attributed to neglect of secondary wave reflections in the present theory.

References

[1] Sychev, V. V., "Three Dimensional Hypersonic Gas Glow Past Slender Bodies at High Angles of Attack," *Journal of Applied Mathematics and Mechanics*, Vol. 24, Aug. 1960, pp. 296-306.

[2] Lighthill, M. J., "Oscillating Aerofoil at High Mach Numbers," *Journal of Aeronautical Sciences*, Vol. 20, June 1953, pp. 402-406.

[3] Appleton, J. P., "Aerodynamic Pitching Derivatives of a Wedge in Hypersonic Flow," *AIAA Journal*, Vol. 2, Nov. 1964, pp. 2034-2036.

[4] Orlik-Rückemann, K. J., "Effect of Wave Reflections on the Unsteady Hypersonic Flow over a Wedge," *AIAA Journal*, Vol. 4, Oct. 1966, pp. 1884-1886.

[5] McIntosh, S.C., Jr., "Studies in Unsteady Hypersonic Flow Theory," Ph.D. Dissertation, Stanford Univ., Calif., Aug. 1965.

[6] Hui, W. H., "Stability of Oscillating Wedges and Caret Wings in Hypersonic and Supersonic Flows," *AIAA Journal*, Vol. 7, Aug. 1969, pp. 1524-1530.

[7] Ericsson, L. E., "Viscous and Elastic Perturbation Effects on Hypersonic Unsteady Airfoil Aerodynamics," *AIAA Journal*, Vol. 15, Oct. 1977, pp. 1481-1490.

[8] Orlik-Rückemann, K. J., "Stabililty Derivatives of Sharp Wedges in Viscous Hypersonic Flow," *AIAA Journal*, Vol. 4, June 1966, pp. 1001-1007.

[9] Mandl, P., "Effect of Small Surface Curvature on Unsteady Hypersonic Flow over an Oscillating Thin Wedge," *C.A.S.I. Transactions*, Vol. 4, No. 1, March 1971, pp. 47-57; see also Errata in *C.A.S.I. Transactions*, Vol. 8, No. 2, 1975, p. 50.

[10] Ghosh, K., "A New Similitude for Aerofoils in Hypersonic Flow," *Proceedings of the 6th Canadian Congress of Applied Mechanics*, Vancouver, Canada, May 29-June 3, 1977, pp. 685-686.

[11] Miles, J. W., "Unsteady Flow at Hypersonic Speeds," *Hypersonic Flow*, Butterworths Scientific Publications, London, England, 1960, pp. 185-197.

J80-190

Flowfield Model for a Rectangular Planform Wing beyond Stall

00001
2001

Allen E. Winkelmann* and Jewel B. Barlow†
University of Maryland, College Park, Md.

Introduction

THE purpose of this Note is to propose a new, general flowfield model for the separated flow over a rectangular planform wing at subsonic speeds and high angles of attack. This model is consistent with earlier observations such as reported in Refs. 1-5, but is primarily inspired by new experimental studies at the University of Maryland. Oil flow studies by Winkelmann et al.[6] have shown strong counter-rotating swirl patterns to occur on reflection plane and full span "two-dimensional" rectangular wings with NACA 0015 and NACA 64_1A211 airfoils in the vicinity of stall. The results of more recent wind tunnel tests (to be reported in this Note) have also shown counter-rotating swirl patterns to exist on stalled finite wings which were free of any direct wall interference effects.

Experiment

Wind tunnel tests were conducted using a series of rectangular planform wings, all with the same 8.89-cm chord 14% Clark Y airfoil section. Primary interest was in the poststall behavior and flowfield. Three test series were completed: 1) a wing model with an aspect ratio $AR = 3.5$ was tested in the 0.46×1.17 m Aerospace Tunnel at a Reynolds number based on a chord of $Re_c = 245{,}000$; 2) a wing model with $AR = 2.86$ was tested in a 0.38×0.38 m student tunnel at $Re_c = 260{,}000$, and 3) a set of wing models with $AR = 3$, 6, 9, and 12 were tested in the 2.36×3.35 m Glenn L. Martin Tunnel at $Re_c = 385{,}000$. Photographs of surface oil flow patterns were obtained in all three cases. Lift, drag, and pitching moment data were taken during the first test series, and a number of exploratory flowfield studies were made during the second test series.

Results

Figure 1 shows a photograph of the oil flow patterns developed on the upper surface of the $AR = 3.5$ wing (test series 1) at an angle of attack $\alpha = 22.8$ deg. The lift coefficient at this point had already gradually rolled off from a maximum at 20.0 deg. A large region of reversed flow is apparent at the central portion of the wing. The oil flows into a pair of counter-rotating swirl patterns and collects in node points. The leading edge separation bubble is highly three-dimensional with the oil tending to form a characteristic "bead-like" pattern.

The "mushroom" shaped three-dimensional separation cell started to develop at $\alpha \simeq 18$ deg with the first signs of trailing edge separation occurring at $\alpha \simeq 15$ deg. The trailing edge stall cell grew in size until, at $\alpha = 26.1$ deg, the surface pattern abruptly changed and the three-dimensional separation line extended to the leading edge. This abrupt change was accompanied by a sudden loss of lift and a noticeable increase in wing buffeting. With increasing α, the counter-rotating swirl patterns were located near the wing tips and a uniformly reversed surface flow existed over most of the span.

Received Aug. 22, 1979; revision received Jan. 2, 1980.

Index categories: Subsonic Flow; Aerodynamics.

*Assistant Professor, Dept. of Aerospace Engineering. Member AIAA.

†Associate Professor and Director, Glenn L. Martin Wind Tunnel, Dept. of Aerospace Engineering. Member AIAA.

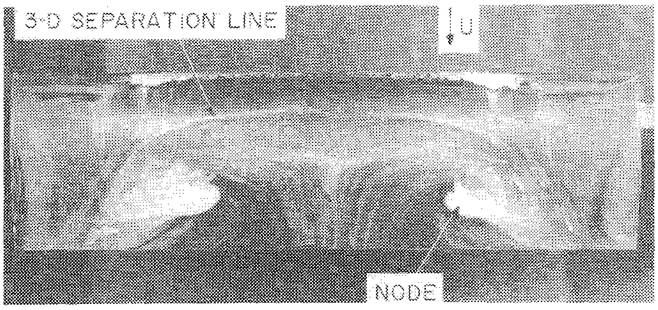

Fig. 1 Oil flow patterns developed on a low aspect ratio wing (14% Clark Y airfoil) at $\alpha = 22.8$ deg, $Re_c = 245,000$.

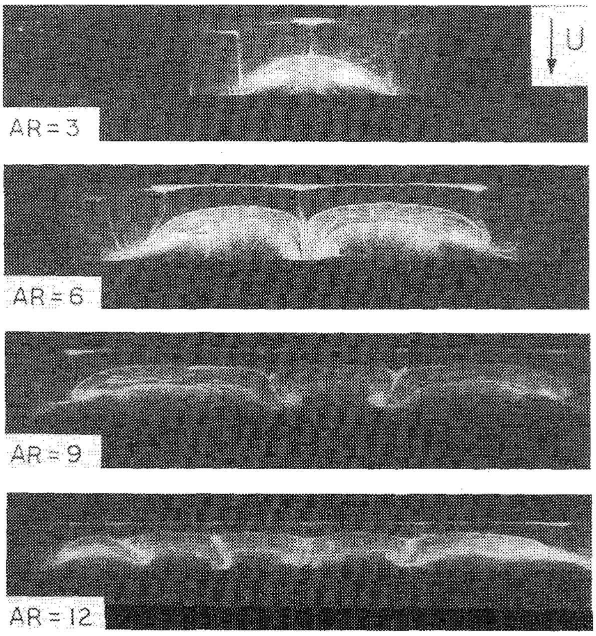

Fig. 2 Oil flow patterns developed on a series of wings (14% Clark Y airfoil) of various aspect ratios; $\alpha = 18.4$ deg, $Re_c = 385,000$.

A number of exploratory flowfield surveys were made during the second test series in attempts to define the flowfield structure associated with the "mushroom" cell. Surveys made with a tuft wand, a water injection probe, and a mini smoke probe indicated that the three-dimensional separation bubble was a closed recirculating region. This was also suggested using the splitter plate technique (Ref. 2). Preliminary surveys using a single element hot-wire probe showed the presence of a highly turbulent wake downstream of the three-dimensional separation bubble.

Figure 2 shows a set of photographs of the four wings ($AR = 3$, 6, 9, and 12) tested in the Glenn L. Martin Tunnel at $\alpha = 18.4$ deg. For aspect ratios above 3, several "mushroom" cells coexist on the upper surface of the wing. As the angle of attack is increased, the cells merge together until only one large cell exists on the wing. For $\alpha \geq 25$ deg, virtually the entire upper surface flow is reversed with the two node points visible very near the wing tips.

A flowfield model based on a tentative analysis of the flow visualization data is shown in Fig. 3 for the low aspect ratio rectangular planform wing just beyond stall. According to this model, the counter-rotating swirl patterns are shown to be produced by the time-averaged effect of a vortex flow that loops from one node point to the other. Along the trailing edge, a secondary vortex rotates in the opposite direction to the loop vortex. The three-dimensional bubble has a rear stagnation line (not shown in Fig. 3) just downstream of the vortex pair. A wake-like flow forms downstream of the three-dimensional bubble. The flow model on the center plane of

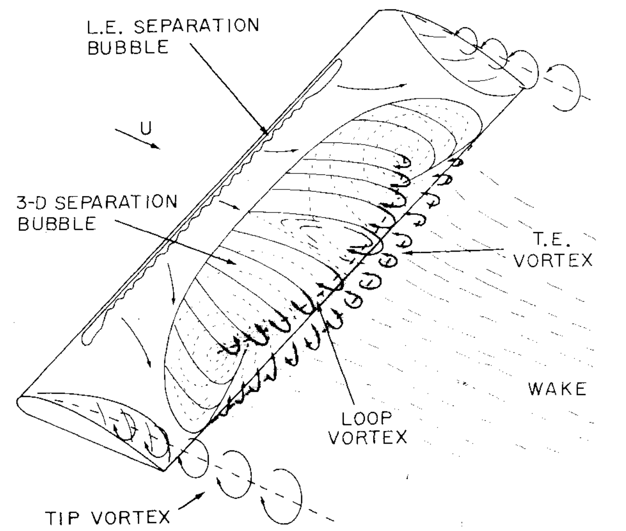

Fig. 3 Tentative flow field model for a low aspect ratio wing just beyond stall.

the wing is essentially the same as the "two-dimensional" model discussed in Ref. 2. The imbedded vortex system is probably quite unsteady in nature. The apparent steady surface flow patterns may actually be caused by the time-averaged effects of an unsteady flowfield. The three-dimensional separation bubble may also contain other secondary vortex systems which are not apparent in the present data. It is conceivable that a separate vortex forms at each node point and continues downstream. However, no evidence was found during the present study to verify such trailing vortices. At high angles of attack, the vortex system spreads across the entire wing and forms node points near the tips. Although the oil flow patterns clearly show the tip vortex and the swirl node separately, some direct interaction between the imbedded vortex system and the tip vortex probably occurs. Eventually, at very high angles of attack, the vortex structure in the three-dimensional separation bubble may burst. Related observations have been reported in Refs. 7 and 8.

The new model for the complex separated flow, as sketched in Fig. 3, should provide additional guidance in preparing future experiments for wings at high angles of attack, and also aid in numerical and/or theoretical modeling of such flows.

Acknowledgments

The work presented herein was supported in part by the NASA Langley Research Center under NASA Contract NSG1570 and in part by a grant from the Minta Martin Fund for Aeronautical Research of the University of Maryland.

References

[1] Prandtl, L., *Essentials of Fluid Dynamics*, Blackie and Son Limited, London, 1952, p. 200 (Fig. 3.83).

[2] Zumwalt, G. W. and Naik, S. N., "A New Flow Model for Highly Separated Airfoil Flows at Low Speed," *Advanced Technology Airfoil Research*, Vol. I, NASA Conference Publ. 2045, Pt. 2, Paper 23, March 1978, pp. 367-382.

[3] Hoad, D. R., "Application of Laser Velocimeter to Airfoil Research," *Advanced Technology Airfoil Research*, Vol. I, NASA Conference Publ. 2045, Pt. 2, Paper 37, March 1978, pp. 559-570.

[4] Kroeger, R. A. and Feistel, T. W., "Reduction of Stall-Spin Entry Tendencies through Wing Aerodynamic Design," SAE Paper 760481, 1976.

[5] Gregory, N., Quincey, V. G., O'Reilly, C. L., and Hall, D. J., "Progress Report on Observations of Three-Dimensional Flow Patterns Obtained during Stall Development on Airfoils and on the Problems of Measuring Two-Dimensional Characteristics," ARC C.P. No. 1146, 1971.

[6] Winkelmann, A. E., Barlow, J. B., Saini, J. K., Anderson, Jr., J. D., and Jones, E., "The Effects of Leading Edge Modifications on the Post-Stall Characteristics of Wings," AIAA Paper 79-0199, Jan. 1980.

[7] Winkelmann, A. E., "Flow Visualization Studies of a Low Aspect Ratio Finite Wing beyond Stall," Dept. of Aerospace Engineering, Univ. of Maryland, College Park, Md., TR AE79-3, Dec. 1979.

[8] Winkelmann, A. E. and Barlow, J. B., "The Effect of Aspect Ratio on Oil Flow Patterns Observed on a Wing beyond Stall," Dept. of Aerospace Engineering, Univ. of Maryland, College Park, Md., TR AE79-4, Dec. 1979.

J 80-191

Improved Version of LTRAN2 for Unsteady Transonic Flow Computations

20005
20009
20019

R. Houwink* and J. van der Vooren†
National Aerospace Laboratory NLR, Amsterdam, The Netherlands

Introduction

IN order to study the aeroelastic characteristics of airplanes flying at transonic speeds, a reliable method of predicting unsteady airloads is required. For a slowly oscillating thin wing section such a prediction can be obtained at relatively low cost using the NASA Ames code LTRAN2.[1] This code solves the low frequency transonic small perturbation (TSP) equation for the velocity potential:

$$[1-M_\infty^2-(\gamma+1)M_\infty^2\phi_x]\phi_{xx}+\phi_{zz}-2M_\infty^2\phi_{xt}=0 \tag{1}$$

derived at a condition $O[k]=O[\delta^{2/3}]=O\ [1-M_\infty^2]\ll 1$ for reduced frequency $k=\omega c/2U_\infty$, relative airfoil thickness δ, and freestream Mach number M_∞. For an airfoil $z=f(x)$ in unsteady motion $z=h(x,t)$, the low frequency airfoil boundary condition is:

$$\phi_z=f_x+h_x \tag{2}$$

on the slit $z=0$, $0<x<1$. The condition in the wake ($z=0$, $x>1$) is given by $\Delta C_p=0$, with for C_p the low frequency expression:

$$C_p=-2\phi_x \tag{3}$$

In applications of the original code,[1] however, Eq. (2) was replaced by the unsteady airfoil boundary condition:

$$\phi_z=f_x+h_x+h_t \tag{4}$$

This is necessary to describe plunge motions.

In this Note it will be shown that the applicability of LTRAN2 is considerably improved at negligible cost if Eq. (3) is also replaced by the unsteady expression for C_p:

$$C_p=-2(\phi_x+\phi_t) \tag{5}$$

The wake condition $\Delta C_p=0$ then correctly describes the downstream vorticity transport in the wake at finite (freestream) velocity.

Equations (4) and (5) and the TSP equation (1) with a slightly modified nonlinear term [the coefficient $(\gamma+1)M_\infty^2$ was replaced by $3-(2-\gamma)M_\infty^2$] have become the basis of a new version (LTRAN2-NLR[2]),which resembles a code developed simultaneously and independently at ONERA.[3] This version is intermediate between the original code[1] and the GTRAN2 code developed by Rizetta and Chin.[4] GTRAN2 is based on Eqs. (4) and (5) and the TSP equation (1) with the additional term $-M_\infty^2\phi_{tt}$, and therefore has no low frequency restriction. In LTRAN2-NLR this ϕ_{tt} term was not added because: 1) it is less effective at low reduced frequencies than the time-derivative terms in Eqs. (4) and (5); and 2) it requires a substantial modification of the original code, leading to a significant increase of computational costs.

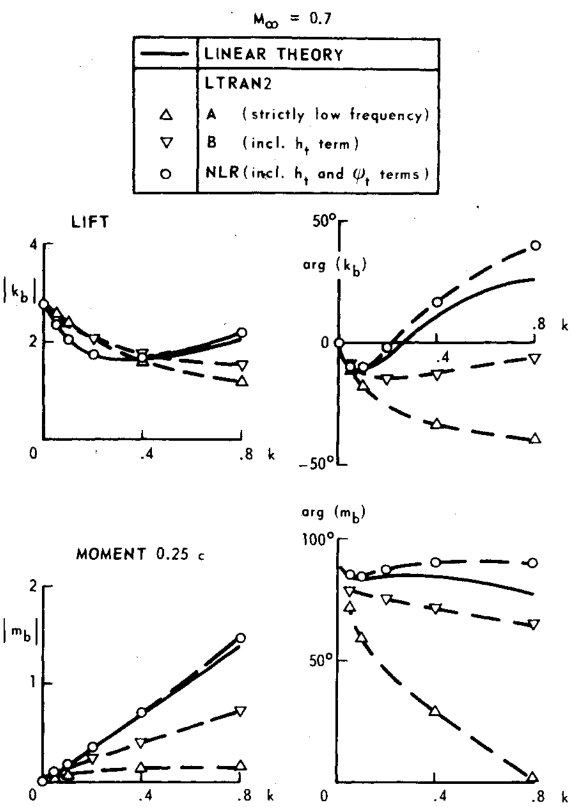

Fig. 1 Unsteady airloads on pitching flat plate showing effect of additional terms.

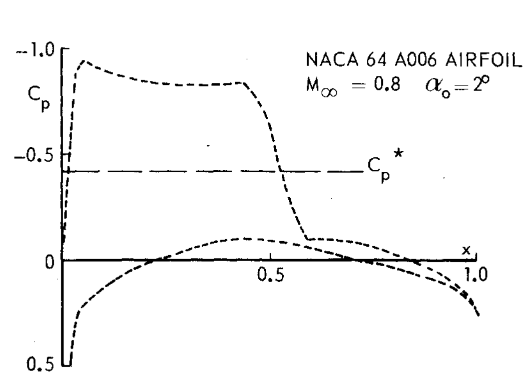

Fig. 2 Steady pressure distribution.

Presented as Paper 79-1553 at the AIAA 12th Fluid and Plasma Dynamics Conference, Williamsburg, Va., July 23-25, 1979; submitted Aug. 27, 1979, revision received Dec. 26, 1979.

Index categories: Nonsteady Aerodynamics; Transonic Flow; Computational Methods.

*Research Engineer, Dept. of Fluid Dynamics.
†Senior Research Engineer, Dept. of Applied Mathematics.